Available online at www.sciencedirect.com
SCIENCE DIRECT
Chemical Engineering and Processing 45 (2006) 383–391
Chemical Engineering and Processing
www.elsevier.com/locate/cep

Composition measurements of crude oil and process water emulsions using thick-film ultrasonic transducers

Guangtian Meng [a], Artur J. Jaworski [a,*], Neil M. White [b]

[a] School of Mechanical, Aerospace and Civil Engineering, The University of Manchester P.O. Box 88, Sackville Street, Manchester M60 1QD, UK
[b] School of Electronics and Computer Science, University of Southampton, Southampton SO17 1BJ, UK

Received 27 May 2005; accepted 12 October 2005
Available online 1 December 2005

Abstract

This paper presents an experimental study to investigate the suitability of thick-film ultrasonic transducers for composition measurements in heterogeneous mixtures. Following on from earlier developments [G. Meng, A.J. Jaworski, T. Dyakowski, J.M. Hale, N.M. White, Design and testing of a thick-film dual-modality sensor for composition measurements in heterogeneous mixtures, Meas. Sci. Technol. 16(4) (2005) 942–954], focused on the design and preliminary testing of the transducers for mixtures of vegetable oil and salty water, the current paper looks in more detail into their application to industrially relevant fluids, namely crude oil and process water, which are common in oil and gas extraction and petrochemical industries. The measurements are based on the time-of-flight of the ultrasonic pressure wave in order to obtain the speed of sound. The results, showing the variation of the speed of sound with the volume fraction of crude oil, for three different temperatures, are compared with five theoretical models available in the existing literature. It is shown that the models proposed by Urick [R.J. Urick, A sound velocity method for determining the compressibility of finely divided substances, J. Appl. Phys. 18 (1947) 983–987] and by Kuster and Toksöz [G.T. Kuster, M.N. Toksöz, Velocity and attenuation of seismic waves in two-phase media. Part I. Theoretical formulations, Geophysics 39 (1974) 587–606] provide a relatively accurate prediction for the speed of sound in the media studied. Interestingly, the model developed by Povey and co-workers [V.J. Pinfield, M.J.W. Povey, Thermal scattering must be accounted for in the determination of adiabatic compressibility, J. Phys. Chem. B 101 (1997) 1110–1112] only agrees with experiment when its thermal scattering features are neglected. Overall, the results obtained demonstrate that the slim-line and compact thick-film transducers can be considered as a viable means for the composition measurements in the process conditions.

Keywords: Heterogeneous mixtures; Oil–water emulsions; Composition measurement; Thick-film technology; Ultrasonic time-of-flight

1. Introduction and literature review

A reliable measurement of the composition of oil–water mixtures and emulsions within the process environment is one of the challenging problems in the oil and gas extraction and petrochemical industries. It is important for reasons which, among others, include monitoring of the inventory and quality of petroleum products, ensuring the desired operating regime of the process plant, which may depend on spatial and temporal distribution of phases in the mixed state, or identifying the environmental hazards such as discharge of oily water into the environment. As an example, a detailed discussion of the needs for identification of the oil–water phase content in the primary separation systems, common within oil and gas extraction industry, is given in Ref. [5].

There are a number of techniques available to measure the phase content of oil–water mixtures. These vary from relatively simple off-line methods of sampling and establishing the volumetric content by gravity or centrifugal separation, to more sophisticated on-line and in situ methods relying on the interaction of particular "sensing fields" (such as ultrasonic, optical, electrical, microwave, X-ray or gamma-radiation, etc.) with matter, which allows to deduce the phase content indirectly. Some more detailed discussions of these methods can be found in edited works such as Refs. [6,7].

The ultrasonic measurement technique has been widely used for characterising heterogeneous mixtures in industrial processes. Its main advantage lies in the ability to rapidly and non-destructively analyse the mixtures that are optically opaque and unlike X-ray or gamma-ray densitometry does not pose risks

* Corresponding author. Tel.: +44 161 275 4352; fax: +44 870 130 7474.
E-mail address: artur.jaworski@manchester.ac.uk (A.J. Jaworski).

0255-2701/$ – see front matter © 2005 Elsevier B.V. All rights reserved.
doi:10.1016/j.cep.2005.10.004

to human health. A brief history of the applications and theoretical developments of ultrasonics is given in Ref. [1]. In the context of ultrasonic composition measurements in oil–water mixtures, it is perhaps worth mentioning Tavlarides and co-workers [8,9], who conducted investigations into monitoring the dispersed volume fraction, in liquid–liquid column extractors and stirred vessels and developed a modified time-average model for the volume fraction calculations.[1] Chanamai et al. [10] investigated the influence of temperature on the ultrasonic properties of oil-in-water emulsions. Nounah et al. [11] developed a low-frequency, near-field method for characterisation of mixtures of non-miscible liquids. More recently, Carlson [12][2] developed an ultrasonic attenuation measurement technique for measuring solids mass fraction in solids–liquid flow by using ultrasonic attenuation technique and by applying an array of transmitters and receivers. Perhaps the most extensive use of ultrasonic methods has been reported in the applications related to food industry, notably by the group of Prof. Povey at the University of Leeds [13,14].

2. Background of the current work

The measurements described in the current paper utilise a well-proven technique of ultrasonic time-of-flight. The novelty of the work, however, lies in the application of the custom made thick-film ultrasonic transducers having a layer thickness of around 50–100 μm and a typical aperture area of 10 mm × 10 mm, deposited onto a 635 μm thick alumina substrate. It is believed that the size and the material characteristics of such sensors may be beneficial for constructing slim-line and robust probes, or sensors which can be potentially easily embedded and distributed within the process environment—in particular, within the oil and gas extraction plant, which was envisaged as the main application area. The design philosophy behind these sensors and the detailed design and fabrication procedures were already reported in [1] and will not be repeated here.

However, the sensors developed for the study underwent only preliminary tests in the mixtures of vegetable oil and salty water (with the NaCl content of 20% by weight for high "contrast"), which are far from being representative media for any practical applications. This is why it has now been decided to conduct additional testing for more industrially relevant media: namely, the mixtures of crude oil and process water. In addition, previous work focused on the construction a "dual-modality" sensor, which enables both the electrical and ultrasonic characterisation of the mixtures. It became apparent, however that, while being generally useful, the electrical characterisation of the mixed fluids was far more difficult and less reliable and repeatable than the measurements provided by the ultrasonic measurement modality of the sensors. Therefore, the current investigation was narrowed down to focus on ultrasonic measurements.

The paper is divided into two main sections: experimental, and results and discussion. The latter contains a comparison between the experimental results obtained (presented in terms of the speed of sound as a function of the oil volume fraction for three temperatures considered) and several literature models that predict the speed of sound within heterogeneous mixtures. This is followed by some general conclusions regarding the application of thick-film ultrasonic transducers for composition measurements. It is hoped that the work presented here will be of benefit to practising process and chemical engineers by highlighting the potential of this new sensor technology.

3. Experimental

3.1. Thick-film sensor and experimental setup

In brief, the fabrication of thick-film sensors involves successive screen-printing and high temperature firing of thick-film pastes [1]. These form a multilayer sandwich of two metallic electrodes (each around 10 μm thick) with piezo-ceramic material (about 50 μm thick) placed in between the electrodes, deposited on an alumina substrate. The overall structure acts as an ultrasonic transducer. During the earlier studies, a number of transducer designs were developed, some of them for pure ultrasonic measurements (Fig. 1a), some of them for

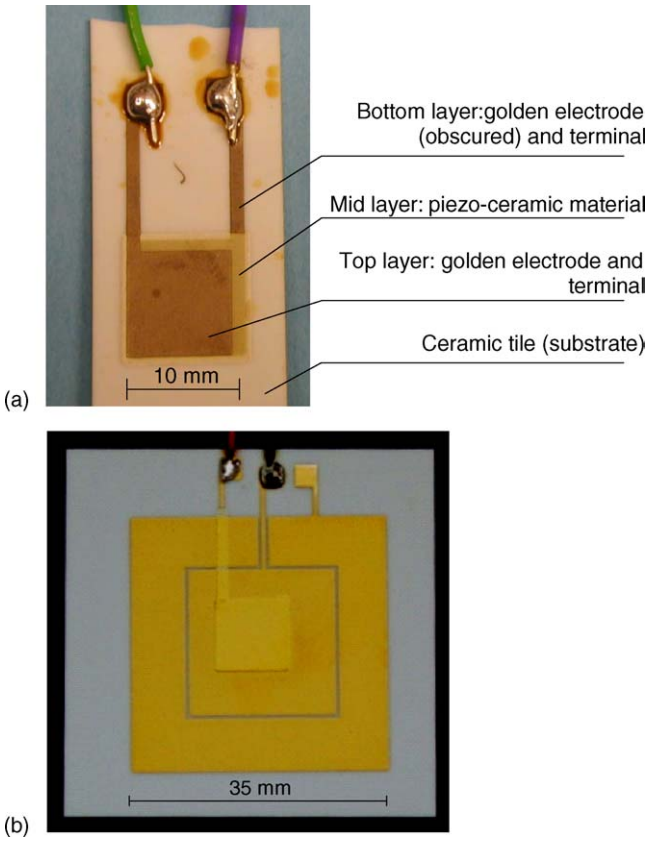

Fig. 1. Thick-film transducers used in the study: (a) ultrasonic transducer and (b) transducer variation enabling ultrasonic and electrical measurements.

[1] See also the prior references by Tavlarides and co-workers cited in Refs. [8] and [9].

[2] The doctoral thesis contains a number of papers (not cited here separately) that arose during the work conducted.

combined ultrasonic and electrical measurements (Fig. 1b). Of course, from the ultrasonic measurement viewpoint these are functionally identical, as it is the middle part, approximately 10 mm × 10 mm, containing piezo-ceramic material, which is responsible for generation and detection of an ultrasonic pulse used for speed of sound measurements.

The experimental setup is similar to that described in Ref. [1], except that the LCR meter for electrical measurements was not used, and there was no need to use surfactants to stabilise the mixtures. A pair of ultrasonic sensors was incorporated into a small measurement "cell" comprising two identical transducers (one "sender", one "receiver") facing one another and located at a distance of 12 mm. Although such a small distance has adverse effects on accuracy of measurements, as discussed in what follows, it was dictated by potential applications, which may require compactly designed probes to fit small process fittings (e.g. in the range below 1 in. diameter). During the measurements, the cell was inserted into a 500 ml beaker containing the oil–water mixtures with oil content between 0 and 100% in 10% intervals, prepared using a high-shear homogeniser. The measurements were performed at 25, 40 and 55 °C to cover a similar range as before.

A Malvern Mastersizer with 630 nm helium/neon laser (with a working range between 0.1 and 1000 μm) was used to measure the drop size distribution. In the current study, the measurements could not be as detailed and accurate as reported previously in [1] due to the fact that crude oil is optically opaque. Therefore, it was difficult to measure the size distribution for realistic oil concentrations due to the high "optical obscuration". Fig. 2a and b shows two selected measurements for oil concentrations of 10 and 1%, respectively. For 10% case the obscuration level was 99.0%, which makes the measurement suspicious. For 1% case (10-fold diluted sample, which produced obscuration of only 48.9%) the drop size distribution is different (with the peak around 80 μm). However, it is not clear as to what extent the dilution itself and the subsequent circulation of the sample within the measurement loop distorts the actual size distribution. Judging from Fig. 2, it is perhaps safe to assume that the droplet sizes broadly fall into the region between a few and up to over a hundred micrometers, which should ensure that the scattering models referred to later are used within the limits of their applicability [1].

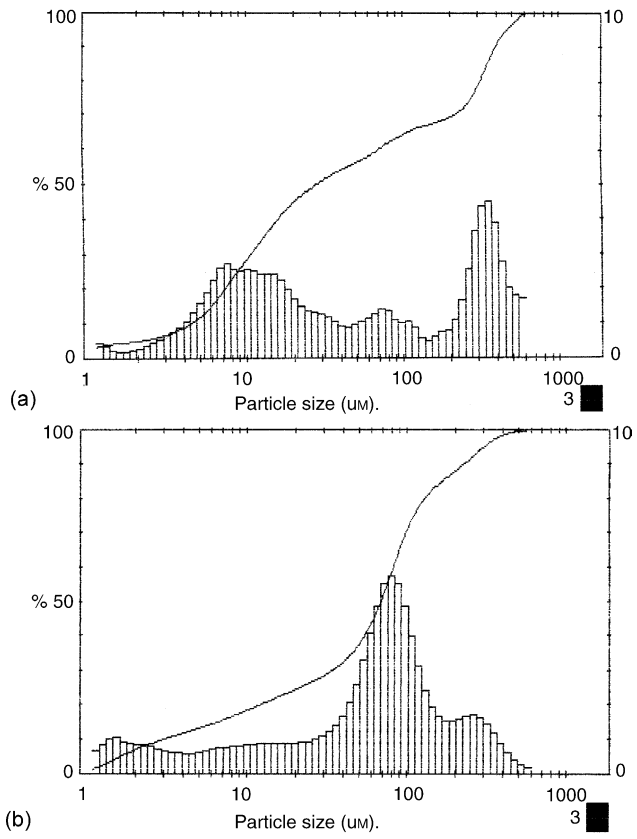

Fig. 2. Sample measurements of the drop size distribution in the samples containing 10% (a) and 1% (b) of crude oil.

3.2. Media properties, calibration procedures and accuracy

The emphasis of the current work was placed on the application of as representative process fluids as possible, in order to qualify the thick-film transducers for composition measurements. To this end, a sample of crude oil was obtained from the National Engineering Laboratory (TUV NEL Ltd.), in Glasgow. This was a mixture of Forties and Beryl crude oil, topped to remove light ends and increase the flashpoint to 75 °C, with kerosene added to restore original viscosity [15]. The process water, which typically contains mixtures of salts of heavy metals, was replaced in this study, for health and safety reasons, by simulated water, in accordance with NEL guidelines [15]. This was a solution of magnesium sulphate $MgSO_4{\cdot}7H_2O$ in distilled water with concentration of 75 kg/m^3. Table 1 lists some properties of the two fluids used, as a function of temperature, which will be useful in theoretical formulae used later.

The density, ρ, was both calculated from the polynomial formula supplied with the media and measured (the difference between measured and calculated values was negligible):

$$\rho_{\text{water}} = -7.95613 \times 10^{-5}T^3 + 3.29456 \times 10^{-3}T^2 - 3.00872 \times 10^{-1}T + 1.4210 \times 10^3$$

$$\rho_{\text{oil}} = 3.37694 \times 10^{-4}T^2 - 7.06892 \times 10^{-1}T + 8.80964 \times 10^2$$

where temperature, T, must be expressed in °C in order to obtain the density in kg/m^3. The thermal expansion coefficient, β, was calculated from the definition as:

$$\beta = -\frac{1}{\rho}\left(\frac{\partial \rho}{\partial T}\right)_P \quad (1)$$

The adiabatic compressibility, κ, was calculated from the basic physics by using measured values of the speed of sound, v, as:

$$\kappa = \frac{1}{v^2\rho} \quad (2)$$

The speed of sound itself was calculated from the time-of-flight of the ultrasonic pulse, but corrected using the known data

Table 1
Selected properties of media used in the experiments

Temperature, T (°C)	Density, ρ (kg/m^3)	Thermal expansion coefficient, β (K^{-1})	Adiabatic compressibility, κ (N/m^2)	Speed of sound, v (m/s)
Crude oil				
25	863.50	7.9908×10^{-4}	5.8582×10^{-10}	1406.0
40	853.23	7.9683×10^{-4}	6.4061×10^{-10}	1352.6
55	843.11	7.9438×10^{-4}	7.0671×10^{-10}	1295.5
Process water				
25	1035.39	2.7557×10^{-4}	4.1199×10^{-10}	1531.1
40	1030.24	4.0690×10^{-4}	3.9580×10^{-10}	1566.0
55	1022.28	6.4609×10^{-4}	3.8524×10^{-10}	1593.5

Table 2
Speed of sound for distilled water [17]

Temperature, T (°C)	Speed of sound in distilled water, v_{dist} (m/s)
25	1496.7
40	1528.9
55	1547.4

for distilled water (shown in Table 2) using the following formula [16]:

$$v = v_{dist}\frac{t_{dist}}{t} \quad (3)$$

where v is the calibrated velocity, v_{dist} is the speed of sound in distilled water, while t_{dist} and t are the measured time-of-flight in distilled water and tested fluids, measured by the pair of thick-film sensors.

The detailed discussion regarding the accuracy of the speed of sound measurements using the experimental setup adopted in this study is given in Ref. [1]. It is worth repeating here that the measurements using thick-film sensors do not use the method of multiple echoes, which can improve the measurement accuracy by the order of magnitude, due to the fact that a relatively weak signal rapidly attenuates within the mixtures under investigation.[3] Instead they rely on a straightforward "pitch-and-catch" technique. In Ref. [1], the measurement error was estimated as ±2 m/s for the sensor spacing of the order of 20 mm and it is reasonable to expect the accuracy of the order of ±4 m/s for the reduced spacing used in the current study. The main difference in expressing the speed of sound data, compared to the previous work, is the application of Eq. (3) to re-calculate the measurements in accordance to the known speeds of sound for distilled water, which of course does not directly affect the measurement accuracy. As an independent check of the combined measurement accuracy and repeatability, three measurements of the speed of sound were taken over a period of 3 months. Standard deviation from the mean value of the speed of sound, Δv, was calculated and the combined error was estimated as $\pm 3\,\Delta v$. This was found to be of within a band of ±0.3%, which for the range of speeds between 1300 and 1600 m/s corresponds to an error of $\pm 3.9 - 4.8$ m/s, congruent with the previous estimates.

[3] Only for the pure substances it is possible to obtain 4–5 "echoes", which of course has a direct impact on improving speed of sound measurements such as expressed in Table 1, making the error within ±1 m/s or better.

4. Results and discussion

Fig. 3 shows the summary of the results obtained during the experimental work. The speed of sound is shown as a function of the oil concentration for three selected temperatures. Error bars corresponding to the estimated error of ±0.3% are shown for each data point. As can be seen, the speed of sound falls monotonically with increasing oil concentration, and, for each temperature, forms a "calibration line", which can be used for predicting the mixture concentration from the ultrasonic propagation data. Of course, due to the fact that the speed of sound for water increases with temperature, while the speed of sound in oil decreases with temperature, the three lines shown in Fig. 3 cross within the range of oil concentrations between 15 and 40%. This behaviour is similar in character to that described by Chanamai et al. [10] for corn oil and distilled water mixtures.

Further work was undertaken to investigate whether the data obtained can be used for validation of some theoretical models of ultrasound propagation, available in the existing literature. These included: (i) time-average model, which is simply equivalent to the sound propagating through a layered arrangement of media, (ii) modified time-average model developed by Tavlarides and co-workers [8,9], (iii) Urick model [2], (iv) model of Kuster and Toksöz [3] and (v) modified Urick model [4]. Table 3

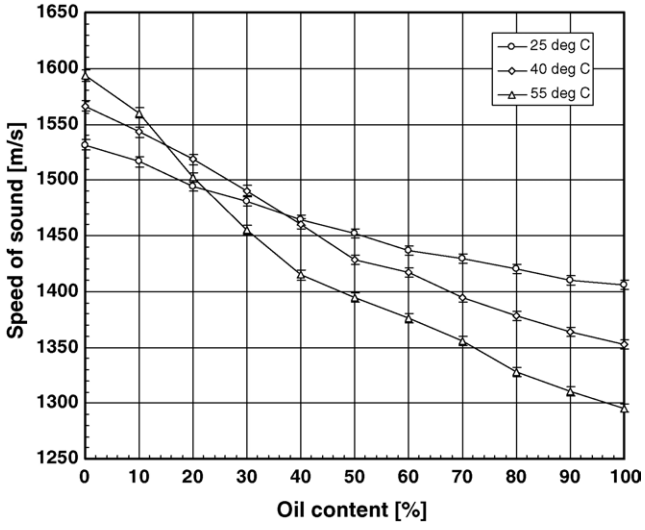

Fig. 3. Measured speed of sound as a function of oil content for 25, 40 and 55 °C.

Table 3
Summary of theoretical models used in this study

Model	Equations defining the model	Main assumptions and/or comments
(i) Time-average model	$\phi = (t^* - t_c)/(t_d - t_c)$	Reflection and refraction effects are neglected
(ii) Modified time-average model, Tavlarides and co-workers [8,9]	$\phi = \dfrac{t^* - t_c}{g_d t_d - g_c t_c}$; $\gamma = \dfrac{\text{speed of sound in dispersed phase}}{\text{speed of sound in continuous phase}}$ For $\gamma \le 1: g_c = 1 + \frac{1}{\gamma^3}[1 - (1-\gamma^2)^{3/2}] - \frac{3}{5\gamma^3}[1 - (1-\gamma^2)^{5/2}] - \frac{2}{5}\gamma^2$, $g_d = \frac{1}{\gamma^2}[1 - (1-\gamma^2)^{3/2}]$ For $\gamma \ge 1: g_c = 1 + \frac{2}{5\gamma^3} - \gamma^2\left[1 - \left(1 - \frac{1}{\gamma^2}\right)^{3/2}\right] + \frac{3}{5}\gamma^2\left[1 - \left(1 - \frac{1}{\gamma^2}\right)^{5/2}\right] - \left(1 - \frac{1}{\gamma^2}\right)^{3/2}$, $g_d = \frac{1}{\gamma^2}$	Reflection and refraction effects are taken into account. Choice of coefficients g_d and g_c depends on the ratio γ and subsequently the model produces two "branches" depending on phase continuity
(iii) Urick model [2]	$v = \frac{1}{\sqrt{\rho_m \kappa_m}}$; $\rho_m = \phi\rho_d + (1-\phi)\rho_c$; $\kappa_m = \phi\kappa_d + (1-\phi)\kappa_c$	The suspended particles are infinitesimally small compared to the wavelength of the sound, and the effects of scattering on the sound velocity may be neglected. Density and compressibility are taken as averages weighted by the phase concentration
(iv) Model of Kuster and Toksöz [3]	$v = \dfrac{1}{\sqrt{\rho^* \kappa_m}}$; $\dfrac{\rho_c - \rho^*}{\rho_c + 2\rho^*} = \phi\dfrac{\rho_c - \rho_d}{\rho_c + 2\rho_d}$; $\kappa_m = \phi\kappa_d + (1-\phi)\kappa_c$	The dispersed particles are solid and spherical; the continuous phase is non-viscous fluid. The wavelengths are much longer than the size of the dispersed particles and multiple scattering effects are negligible. The model produces two "branches" depending on phase continuity
(v) Modified Urick model [4]	$\dfrac{1}{v^2} = \dfrac{1}{v_c^2}(1 + \alpha\phi + \delta\phi^2)$; $\alpha = \left(\dfrac{\kappa_d - \kappa_c}{\kappa_c} + \theta + \dfrac{\rho_d - \rho_c}{\rho_c}\right)$; $\delta = \left(\dfrac{\kappa_d - \kappa_c}{\kappa_c} + \theta\right)\left(\dfrac{\rho_d - \rho_c}{\rho_c}\right) + \dfrac{2(\rho_d - \rho_c)^2}{3\rho_c^2}$; $\theta = (\mu - 1)\dfrac{\rho_d C_{pd}}{\rho_c C_{pc}} R^2$; $R = \left(\dfrac{\beta_d}{\rho_d C_{pd}} - \dfrac{\beta_c}{\rho_c C_{pc}}\right) / \dfrac{\beta_c}{\rho_c C_{pc}}$	Model accounts for the thermal scattering but the long wavelength limit applies. The model produces two "branches" depending on phase continuity

Symbols—ρ_m: the mean density of mixtures; ρ^*: the effective inertial density of the mixture; ρ_c, ρ_d: the density of continuous and dispersed phase, respectively; κ_m: the mean adiabatic compressibility of the mixture; κ_c, κ_d: the adiabatic compressibility of continuous and dispersed phase, respectively; ϕ: the concentration of the dispersed phase; μ: the ratio of the specific heats of continuous phase (C_{pc}/C_{vc}); β_c, β_d: the volume thermal expansivity of continuous and dispersed phase, respectively; C_{pc}, C_{pd}: the specific heat at constant pressure of continuous and dispersed phase, respectively; t^*, t_c, t_d: time of sound travel in the mixture, continuous phase and dispersed phase, respectively; γ: the ratio of the speed of sound in the dispersed phase to the speed of sound in the continuous phase.

summarises models (i)–(v), listing the relevant formulae, symbols and the main assumptions made during the derivation.

Fig. 4 shows the comparison of the experimental data with models (i)–(iv), for the three temperatures considered in this study. Judging from the graphs, it is difficult to select one model that would fit the experimental data best consistently for all temperatures considered. Clearly, model (i) based on the time-average approach is inadequate for modelling the behaviour of oil–water mixtures studied here. This is expected, because it does not consider any scattering effects, which must be significant in highly dispersed media of high concentration of inclusions (droplets). Out of the remaining models, model (iii), also referred to as Urick model [2], and model (iv), developed by Kuster and Toksöz [3] seem to match the experimental data most closely. It is worth pointing out that when plotting the models that produce two separate branches for oil-continuous and water-continuous mixtures, it was tacitly assumed that the phase inversion takes place at the oil content of 50%. This may not be generally true; it is known that mixtures of crude oil and water may undergo such phase inversion between oil content values of 30–70% and that such inversion is a function of thermodynamic conditions. These phenomena could explain the point in Fig. 4c (for oil content 40%) which is clearly well outside of models (iii) and (iv) but seems to coincide with model (ii).

The application of model (v), as described in Ref. [4], to the current work is somewhat more involved. The model takes into account the effects of thermal scattering and requires thermal–fluid data including thermal expansivity, β, and specific heat capacities, C_p and C_v, for both the continuous and dispersed phases (see Table 3). The calculation of thermal expansivity is straightforward (see Table 1), but unfortunately the heat capacities are not available for an arbitrary medium and strictly need to be measured using calorimetric methods. These were not available to the authors, however, it was decided instead to perform a parametric analysis using the widely available data for water and a range of heavier hydrocarbons in order to ascertain whether or not model (v) could give better results than models (i)–(iv).

Table 4 contains the values of specific heat capacities for selected hydrocarbons obtained from Refs. [17–20] and for distilled water [17], at pressure 0.1 MPa. Crude oil such as used

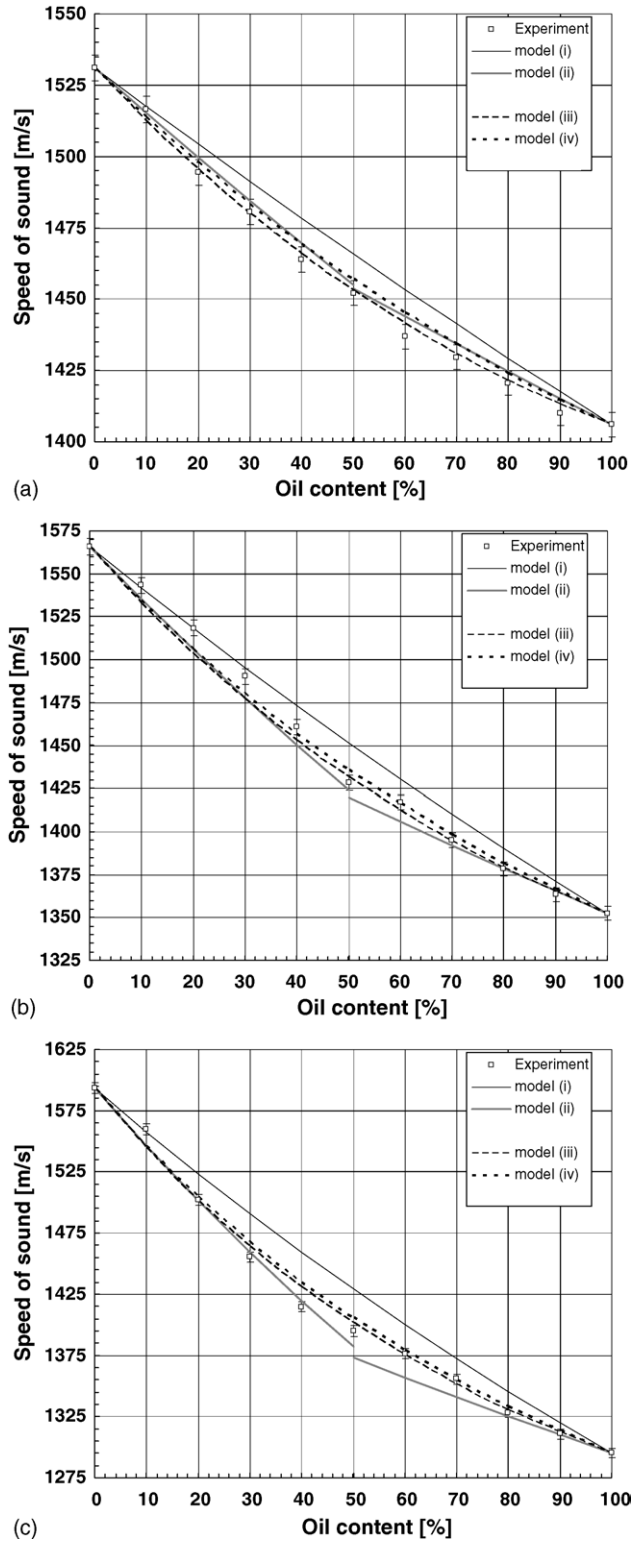

Fig. 4. Comparison between experimental results and models (i)–(iv) for 25 °C (a), 40 °C (b) and 55 °C (c).

in the experiments reported here is usually a mixture of various hydrocarbons and it is expected that its properties will be broadly similar. It can be seen from Table 4 that C_p for hydrocarbons is typically in the range of 2.2–2.4 kJ kg^{-1} K^{-1} while the ratio of the specific heat capacities, μ, is typically in the range 1.18–1.30.

Table 4
Numerical values of specific heat capacities for selected hydrocarbons [17–20] and distilled water [17], at pressure 0.1 MPa

Medium	T (°C)	C_p (kJ kg^{-1} K^{-1})	C_v (kJ kg^{-1} K^{-1})	$\mu = C_p/C_v$
Hexane [17]	25	2.2518	1.7436	1.2915
	40	2.3170	1.7998	1.2874
	55	2.3860	1.8580	1.2842
Heptane [17]	25	2.2405	1.7751	1.2622
	40	2.2990	1.8288	1.2571
	55	2.3610	1.8847	1.2527
n-Pentadecane [18]	30	2.214	1.867	1.1859
	50	2.276	1.918	1.1867
	70	2.348	1.981	1.1853
n-Tetradecane [19]	20	2.198	1.842	1.1933
	40	2.247	1.884	1.1927
	60	2.304	1.937	1.1895
n-Dodecane [20]	20	2.192	1.820	1.2044
	40	2.253	1.872	1.2035
	60	2.318	1.931	1.2004
Distilled water [17]	25	4.1813	4.1376	1.0106
	40	4.1794	4.0734	1.0260
	55	4.1830	4.0016	1.0453

The latter is significant from the viewpoint of model (v) because the magnitude of parameter θ (see Table 3) depends on the magnitude of factor $(\mu - 1)$, which is relatively small for fluids such as distilled water but becomes very large for hydrocarbons discussed here. Fig. 5 shows the experimental data compared with the predictions of model (v) obtained from a parametric study which included values of $C_{p,\mathrm{oil}}$ 2.20, 2.30 and 2.40 kJ kg^{-1} K^{-1} and values of μ_{oil} 1.0, 1.1, 1.2 and 1.3, in order to cover a range indicated in Table 4. $C_{p,\mathrm{water}}$ and μ_{water} were those for distilled water and appropriate values were used for each of the three temperatures. However, an additional calculation was made at each temperature for $\mu_{\mathrm{water}} = 1$ for comparisons.

From Fig. 5, the following observations can be made. Firstly, for the water-continuous mixtures (left hand side of the graphs) the predicted speed of sound is close to the experimental data for $\mu_{\mathrm{water}} = 1$ and departs form the experimental results when the actual value for μ_{water} is used (the only exception is temperature 55 °C where the experimental data and the model prediction are quite close to one another). In addition, when $\mu_{\mathrm{water}} > 1$ there is some sensitivity observed to the change of $C_{p,\mathrm{oil}}$, but it does not seem to be very significant. Secondly, for the oil-continuous mixtures (right hand side of the graphs) the model also agrees very well with the experimental results for $\mu_{\mathrm{oil}} = 1$, but for $\mu_{\mathrm{oil}} > 1$ it rapidly departs from the experimental data. Increase in μ_{oil} leads to theoretical predictions which are progressively lower than experimental results, with some visible effect of the value of $C_{p,\mathrm{oil}}$ when μ_{oil} is kept constant (in the graphs an arrow indicates the direction of increasing C_p). However, it needs to be pointed out that mathematically, for $\mu = 1$, the parameter θ in Table 3 becomes zero and the model itself depends only on the media densities and compressibilities (albeit in a different way than in any of the models (i)–(iv)) and thus the thermal scattering aspect of the theoretical approach is lost. It is easy to

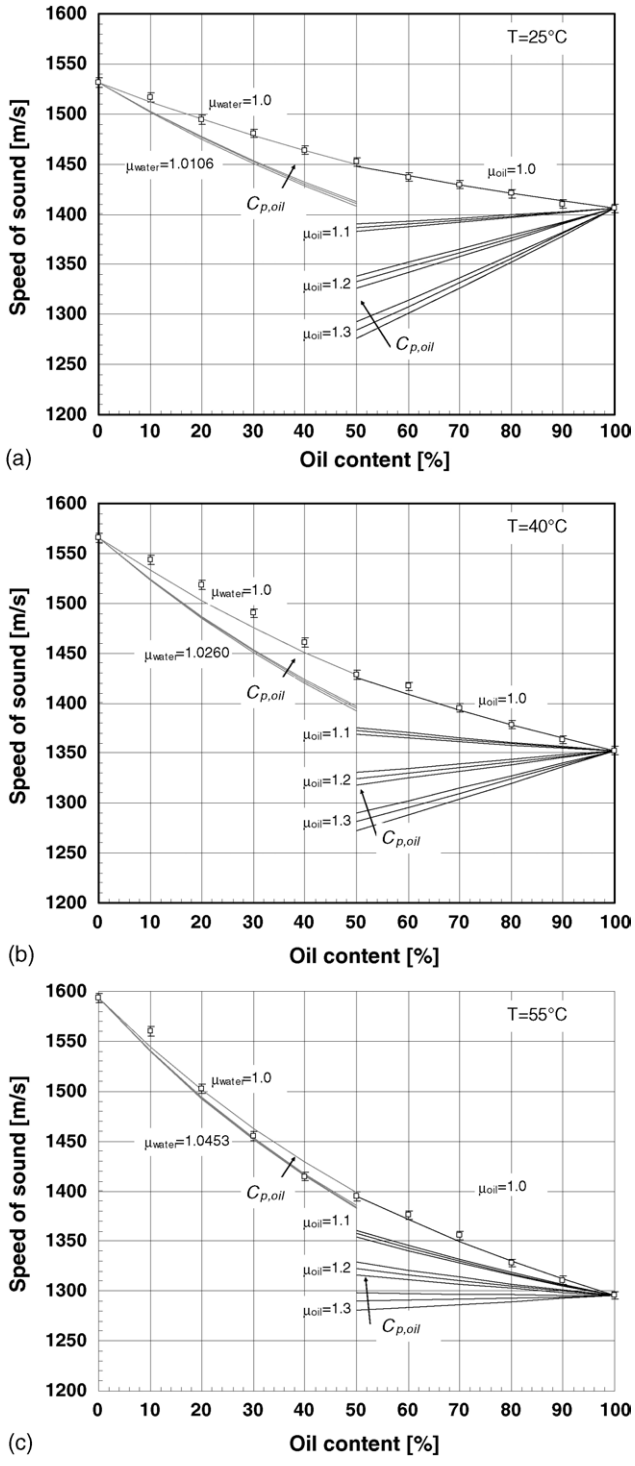

Fig. 5. Results of the parametric study of model (v) involving change of C_p to include values 2.2, 2.3 and 2.4 kJ kg^{-1} K^{-1} and μ to include values 1.0, 1.1, 1.2 and 1.3. Graphs (a–c) correspond to temperatures 25, 40 and 55 °C, respectively. Arrow indicates increase in the value of C_p.

show that for such a "simplified" model (v) the only difference between model (v) and model (iii) is the appearance of the term $2((\rho_d - \rho_c)^2/3\rho_c^2)\phi^2$ in the equation for $(1/v^2)$.[4]

[4] See Appendix A for the detailed derivation.

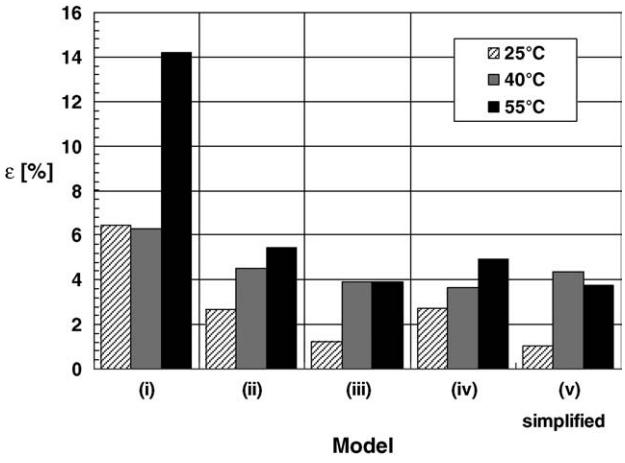

Fig. 6. Illustration of the discrepancy between the experimental data and the theoretical predictions for various models considered at 25, 40 and 55 °C.

To provide a brief summary of the suitability of different models to predict the speed of sound within oil–water mixtures studied in this work, Fig. 6 plots one of the possible measures of the discrepancy between experimental data and theoretical predictions. It is defined here as follows:

$$\varepsilon = \frac{\sum |v_{exp} - v_{theor}|}{v_{mean}} \times 100\% \quad (4)$$

where:

$$v_{mean} = \frac{v_{water} + v_{oil}}{2} \quad (5)$$

The summation in Eq. (4) is carried out over all experimental points considered, i.e. between 0 and 100% oil content in 10% steps. The value of ε is calculated separately for each model and each temperature and plotted in Fig. 6. It is worth pointing out that when model (v) is simplified to include the values of $\mu = 1$, it seems to predict the speed of sound with accuracy comparable with models (iii) and (iv).

5. Conclusion

This paper presents an experimental study, based on the ultrasonic time-of-flight principle, carried out to characterise heterogeneous mixtures (emulsions) of crude oil and process water, using purpose made thick-film ultrasonic transducers. The results demonstrate that these sensors can be used as a simple and reliable method of measuring the composition of industrially relevant heterogeneous mixtures. The paper also provides a short review of the theoretical models of the ultrasonic propagation and studies their relevance to predicting the ultrasonic speed of sound for the media under investigation. It is shown that, out of five models considered, models proposed by Urick [2] and Kuster and Toksöz [3] seem to predict the speed of sound with the best accuracy.

Future work will include two strands of research. Firstly, it is intended to study a wider selection of process media, within much wider process conditions, especially temperature range and pressures. Secondly, it needs to address the transfer of the

measurement technologies developed into the process environment. The latter could, for example, include not only application of various coatings on the sensor surfaces (including glassy substances) for hygienic and longevity reasons, but also needs to include the basic engineering work to enable construction of industrially acceptable probes that could be reliably fitted into the process vessels.

Acknowledgements

The authors would like to gratefully acknowledge the support from EPSRC under the grant number GR/R35858. We would also express our thanks to: Professor Malcolm Povey of University of Leeds for useful discussions regarding theoretical models of ultrasound propagation, Dr. Ming Yang of TUV NEL, Glasgow, for providing the media used in the study, Morgan Electro Ceramics Ltd. for supplying the piezoelectric materials and Mrs. Liz Davenport from the School of CEAS, University of Manchester, for providing expert help with drop size distribution analysis. Guangtian Meng would like to acknowledge the financial support for his postgraduate studies obtained from Oilfield Technology Ltd., the University of Manchester and Universities UK.

Appendix A

One of the Referees requested us to supplement this paper with a clarification as to why model (v) reduces to model (iii) for $\mu = 1$, with exception of the term $2((\rho_d - \rho_c)^2/3{\rho_c}^2)\phi^2$ in the equation for $(1/v^2)$. Starting from Urick equation for the speed of sound, $v = \frac{1}{\sqrt{\rho_m \kappa_m}}$ and substituting ρ_m and κ_m, from Table 3, one obtains:

$$v = \frac{1}{\sqrt{(\phi\rho_d + (1-\phi)\rho_c)(\phi\kappa_d + (1-\phi)\kappa_c)}} \tag{A.1}$$

From basic physics the speed of sound in the continuous phase is

$$v_c = \frac{1}{\sqrt{\rho_c \kappa_c}} \tag{A.2}$$

Dividing equation (A.2) by (A.1), raising both sides to the power of 2, and making a series of straightforward algebraic transformation one arrives at the following:

$$\begin{aligned}\frac{v_c^2}{v^2} &= \frac{(\phi\rho_d + (1-\phi)\rho_c)(\phi\kappa_d + (1-\phi)\kappa_c)}{\rho_c\kappa_c} \\ &= \frac{((\rho_d - \rho_c)\phi + \rho_c)((\kappa_d - \kappa_c)\phi + \kappa_c)}{\rho_c\kappa_c} \\ &= \frac{\rho_c\kappa_c + (\kappa_c(\rho_d - \rho_c) + \rho_c(\kappa_d - \kappa_c))\phi + (\rho_d - \rho_c)(\kappa_d - \kappa_c)\phi^2}{\rho_c\kappa_c} \\ &= 1 + \left(\frac{\rho_d - \rho_c}{\rho_c} + \frac{\kappa_d - \kappa_c}{\kappa_c}\right)\phi + \left(\frac{\rho_d - \rho_c}{\rho_c}\right)\left(\frac{\kappa_d - \kappa_c}{\kappa_c}\right)\phi^2\end{aligned}$$

Hence

$$\frac{1}{v^2} = \frac{1}{v_c^2}\left(1 + \left(\frac{\kappa_d - \kappa_c}{\kappa_c} + \frac{\rho_d - \rho_c}{\rho_c}\right)\phi + \left(\frac{\kappa_d - \kappa_c}{\kappa_c}\right)\left(\frac{\rho_d - \rho_c}{\rho_c}\right)\phi^2\right) \tag{A.3}$$

or more simply (introducing α_1 and δ_1 as coefficients in front of ϕ and ϕ^2 terms, respectively):

$$\frac{1}{v^2} = \frac{1}{v_c^2}\left(1 + \alpha_1\phi + \delta_1\phi^2\right) \tag{A.4}$$

Modified Urick equation (v), on the other hand, is expressed as follows:

$$\frac{1}{v^2} = \frac{1}{v_c^2}\left(1 + \alpha\phi + \delta\phi^2\right) \tag{A.5}$$

where α and δ are defined in Table 3. By looking at the form of these coefficients it is clear that when $\mu = 1$, θ becomes zero. Subsequently, $\alpha = \alpha_1$ while $\delta = \delta_1 + 2((\rho_d - \rho_c)^2/3{\rho_c}^2)$ which completes the proof.

References

[1] G. Meng, A.J. Jaworski, T. Dyakowski, J.M. Hale, N.M. White, Design and testing of a thick-film dual-modality sensor for composition measurements in heterogeneous mixtures, Meas. Sci. Technol. 16 (4) (2005) 942–954.
[2] R.J. Urick, A sound velocity method for determining the compressibility of finely divided substances, J. Appl. Phys. 18 (1947) 983–987.
[3] G.T. Kuster, M.N. Toksöz, Velocity and attenuation of seismic waves in two-phase media. Part I. Theoretical formulations, Geophysics 39 (1974) 587–606.
[4] V.J. Pinfield, M.J.W. Povey, Thermal scattering must be accounted for in the determination of adiabatic compressibility, J. Phys. Chem. B 101 (1997) 1110–1112.
[5] A.J. Jaworski, T. Dyakowski, Measurements of oil–water separation dynamics in primary separation systems using distributed capacitance sensors, Flow Meas. Instrum. 16 (2–3) (2005) 113–127.
[6] E. Kress-Rogers, C.J.B. Brimelow (Eds.), Instrumentation and Sensors for the Food Industry, Woodhead Publishing Limited, Cambridge, UK/CRC Press, LLC, Boca Raton, USA, 2001.
[7] R.A. Williams, M.S. Beck (Eds.), Process Tomography: Principles, Techniques and Applications, Butterworth-Heinemann, Oxford, UK, 1995.
[8] C. Tsouris, L.L. Tavlarides, Volume fraction measurements of water in oil by an ultrasonic technique, Ind. Eng. Chem. Res. 32 (1993) 998–1002.
[9] C. Tsouris, M.A. Norato, L.L. Tavlarides, Pulse-echo ultrasonic probe for local volume fraction measurements in liquid–liquid dispersions, Ind. Eng. Chem. Res. 34 (1995) 3154–3158.
[10] R. Chanamai, J.N. Coupland, D.J. McClements, Effect of temperature on the ultrasonic properties of oil-in-water emulsions, Colloids Surf. A: Physicochem. Eng. Aspects 139 (1998) 241–250.
[11] H. Nounah, J.Y. Ferrandis, B. Cros, G. Levêque, A. Moudden, Acoustic near-field process for the characterization of non-miscible liquids, Sens. Actuators B 59 (1999) 48–53.
[12] J. Carlson, Ultrasonic characterization of materials and multiphase flows, Doctoral Thesis of Lulea University of Technology, Department of Computer Science and Electrical Engineering, Sweden, 2002.
[13] M.J.W. Povey, Ultrasonics of food, Contemporary Phys. 39 (1998) 467–478.
[14] P.V. Nelson, M.J.W. Povey, Y. Wang, An ultrasound velocity and attenuation scanner for viewing the temporal evolution of a dispersed phase in fluids, Rev. Sci. Instrum. 72 (11) (2001) 4234–4241.

[15] National Engineering Laboratory, A Guide to the NEL Multiphase Flow Facility, TUV NEL Ltd., 2004.
[16] G. Douheret, M.I. Davis, J.C.R. Reis, I.J. Fjellanger, M.B. Vaage, H. Hoiland, Aggregative processes in aqueous solutions of isomeric 2-butoxyethanols at 298.15 K, Phys. Chem. Chem. Phys. 4 (24) (2002) 6034–6042.
[17] US National Institute of Standards and Technology, NIST Chemistry Web Book—NIST Standard Reference Database Number 69, March 2003 release (http://webbook.nist.gov/chemistry/fluid/).
[18] D.V. Dovnar, Y.A. Lebedinskij, T.S. Khasanshin, A.P. Shchemelev, The thermodynamic properties of *n*-pentadecane in the liquid state, determined by the results of measurements of sound velocity, High Temp. 39 (6) (2001) 835–839 (translated from Teplofizika Vysokikh Temperatur 39 (6) 899–904).
[19] T.S. Khasanshin, A.P. Shchemelev, The thermodynamic properties of *n*-tetradecane in liquid state, High Temp. 40 (2) (2002) 207–211 (translated from Teplofizika Vysokikh Temperatur, 40 (2) 235–240).
[20] T.S. Khasanshin, A.P. Shchamialiou, O.G. Poddubskij, Thermodynamic properties of heavy *n*-alkanes in the liquid state: *n*-dodecanel, Int. J. Thermophys. 24 (5) (2003) 1277–1289.